

## NUCLEON AND HYPERON RESONANCES WITH THE CRYSTAL BALL

W.J. BRISCOE, A. SHAFI, AND I.I. STRAKOVSKY

*Department of Physics and Center for Nuclear Studies  
The George Washington University, Washington, DC 20052, USA  
E-mail: briscoe@gwu.edu*

### THE CRYSTAL BALL COLLABORATION

*Abilene Christian University, Argonne National Laboratory,  
Arizona State University, Brookhaven National Laboratory,  
University of California at Los Angeles, University of Colorado,  
George Washington University, Universität Karlsruhe,  
Kent State University, University of Maryland,  
Petersburg Nuclear Physics Institute, University of Regina,  
Rudjer Boskovic Institute and Valparaiso University*

The Crystal Ball Spectrometer is being used at Brookhaven National Laboratory in a series of experiments which study all neutral final states of  $\pi^-p$  and  $K^-p$  induced reactions. We report about the experimental setup and progress in obtaining new results for the radiative capture reactions  $\pi^-p \rightarrow \gamma n$  and  $K^-p \rightarrow \gamma \Lambda$ , charge exchange  $\pi^-p \rightarrow \pi^0 n$ , two  $\pi^0$  production  $\pi^-p \rightarrow \pi^0 \pi^0 n$ , and  $\eta$  production  $\pi^-p \rightarrow \eta n$  reactions. Data have also been obtained on the decays of  $N^*$ ,  $\Delta$ ,  $\Lambda$ , and  $\Sigma$  resonances. Threshold  $\eta$  production has been studied in detail for both  $\pi^-p$  and  $K^-p$ . Sequential resonance decays have been investigated by studying the  $2\pi^0$  production mechanism both in the fundamental interaction and in nuclei. In addition, we have used the  $\eta$ s produced near threshold to make precision measurements searching in particular for rare and forbidden  $\eta$  decays.

### 1. Introduction

Quantum Chromodynamics, QCD, attempts to explain the strong interaction in terms of the underlying quark and gluon degrees of freedom. The study of the structure of baryons and their excitations in terms of the elementary quark and gluon constituents is thus pivotal to our understanding of nuclear matter within QCD. It is the major goal of Nuclear Physics to understand the strong interaction and keeping this goal in mind motivates our choice of the particular reactions of interest that we selected to study

with the Crystal Ball at BNL. We will describe these measurements below, but first we look at the experimental conditions at BNL.

## 2. The BNL Experimental Setup

### 2.1. *The Crystal Ball*

We used the SLAC Crystal Ball in the C6 line at the Brookhaven National Laboratory, BNL, Alternating Gradient Synchrotron, AGS, with pion and kaon momenta up to 760 MeV/c. Data are taken simultaneously on all reactions for each incident particle; this helps ensure us that background events are accurately subtracted and also allows us to normalize reactions with smaller cross sections to more well determined reactions. Data taking using the Crystal Ball began in July 1998 and continued until late November 1998. A second period of data taking occurred in May 2002.

The Crystal Ball is a segmented, electromagnetic, calorimetric spectrometer, covering 94% of  $4\pi$  steradians. It was built at SLAC and used for meson spectroscopy measurements there for three years. It was then used at DESY for five years of experiments and put in storage at SLAC from 1987 until 1996 when it was moved to BNL by our collaboration.

The Crystal Ball is constructed of 672 hygroscopic NaI crystals, hermetically sealed inside two mechanically separate stainless steel hemispheres. The crystals are viewed by photomultipliers, PMTs. There is an entrance and exit tunnel for the beam, LH<sub>2</sub> target plumbing, and veto counters.

The crystal arrangement is based on the geometry of an icosahedron (20 triangular faces or “major-triangles” arranged to form a spherical shape.) Each “major-triangle” is subdivided into four “minor-triangles”, which in turn consist of nine individual crystals. Each crystal is shaped like a truncated triangular pyramid, points towards the interaction point, is optically isolated, and is viewed by a PMT which is separated from the crystal by a glass window. The beam pipe is surrounded by 4 scintillators covering 98% of the target tunnel (these scintillators form the veto-barrel.)

This high degree of segmentation provides excellent resolution. Electromagnetic showers in the Crystal Ball are measured with an energy resolution of  $\sigma/E = 2.7\%/E[GeV]^{1/4}$ . Shower directions are measured with a resolution in  $\theta$  of  $\sigma = 2^\circ\text{--}3^\circ$  for photon energies in the range 50–500 MeV; the resolution in  $\phi$  is  $2^\circ/\sin\theta$ . Typically, 98% of the deposited energy of each photon is contained in a cluster of thirteen crystals (a crystal with its twelve nearest neighbors). The thickness of the NaI amounts to nearly one hadron interaction length resulting in two-thirds of the charged pions

interacting in the detector. The minimum ionization energy deposited is 197 MeV; the length of the counters corresponds to the stopping range of 233 MeV for  $\mu^\pm$ , 240 MeV for  $\pi^\pm$ , 341 MeV for  $K^\pm$ , and 425 MeV for protons. The preliminary energy calibration is performed using the 0.661 MeV  $\gamma$ 's from a  $^{137}\text{Cs}$  source. The final energy calibration is done using three reactions: i)  $\pi^-p \rightarrow \gamma n$  at rest, yielding an isotropic, monochromatic  $\gamma$  flux of 129.4 MeV; ii)  $\pi^-p \rightarrow \pi^0 n$  at rest, yielding a pair of photons in the energy range 54.3–80 MeV, almost back to back; and iii)  $\pi^-p \rightarrow \eta n$  at threshold, yielding two photons, about 300 MeV each, in coincidence almost back to back. The PMT analog pulses are sent to ADCs for digitization. Analog sums of the signals from each minor-triangle are available for trigger purposes.

In addition to the expected high efficiency for photons, the Crystal Ball is also fairly responsive to neutrons. We were able to measure the response of the NaI(Tl) to neutrons by using the reaction  $\pi^-p \rightarrow \pi^0 n$  and kinematics to determine the efficiency (as high as 40%) as a function of energy.<sup>1</sup>

## 2.2. Beam Line

Figure 1 shows the experimental setup at BNL on the C6 beam line. The final stages of the C6 beamline consist of four quadrupoles and a dipole that form a beam momentum spectrometer. Wire chambers are located on both sides of the dipole to track the particles through the spectrometer. The momentum resolution is 0.3%. The scintillators located up and down stream of the dipole provide TOF information and the coincidence trigger for the beam. Scintillators surround the LH2 target to provide a charged particle veto. Two columns of scintillator neutron counters are located downstream of the Crystal Ball. A beam veto scintillator is located further downstream. A concrete shield wall located upstream of the beam stop shields the Crystal Ball from low energy photons from the stop. A Čerenkov counter is located just after this wall to monitor electron contamination in the beam.

The usual trigger consists of: a beam coincidence trigger, no downstream beam veto, and a total energy-over-threshold signal from the Crystal Ball. The trigger is normally set on the total energy level. A trigger based on the distribution of the energy in different regions of the Crystal Ball was also used to provide a more restrictive trigger in certain cases.

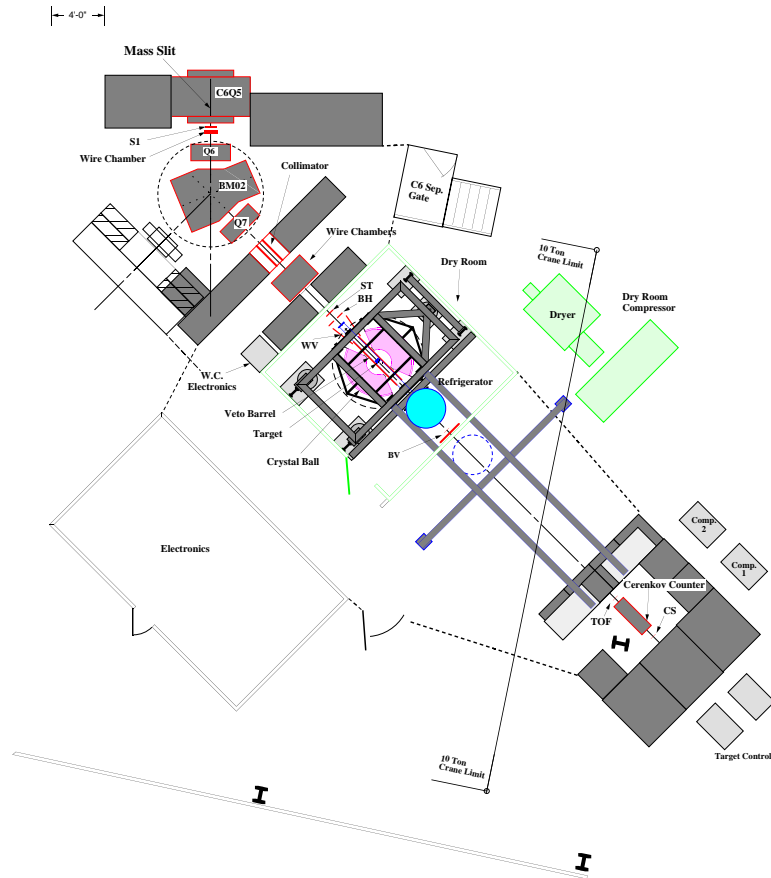


Figure 1. Experimental setup at the BNL AGS C6 line.

### 3. Pion-Induced Reactions

#### 3.1. Radiative Capture

The radiative decay of a resonance provides the ideal laboratory for testing theories of the strong interaction, gives us insight into the fundamental interactions between mesons and nucleons, and allows us to probe into the structure of the nucleon itself. In particular, these data are important in the study of the radiative decay of the neutral Roper resonance. They can be combined with recent JLab Hall B data for the reactions  $\gamma p \rightarrow \pi^+ n$  and

$\gamma p \rightarrow \pi^0 p$  which study the mesonic decays of the charged Roper resonance in the incident photon energy region from 400 to 700 MeV. In addition, comparison of our data to the new JLab data taken on the inverse reaction  $\gamma n \rightarrow \pi^- p$ , using a deuteron target,<sup>2</sup> tests extrapolation techniques for the deuteron correction and study medium effects within the deuteron.

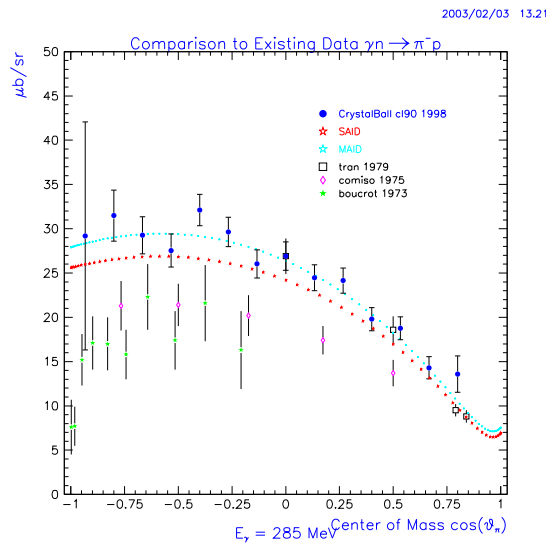


Figure 2. The radiative capture differential cross section (plotted in the photoproduction channel) at a photon energy of 285 MeV - a pion beam momentum of 238 MeV/c. The normalization factor was obtained from the CEX - the effective beam flux was identical for both these measurements (the same data run was analyzed for the charge exchange as well as the radiative capture channels). In this plot we also include previous data,<sup>3, 4, 5</sup> and the SAID<sup>6</sup> as well as MAID<sup>7</sup> predictions.

Figure 2 shows the radiative capture differential cross section (plotted in the photoproduction channel) at a photon energy of 285 MeV which corresponds to a pion beam momentum of 238 MeV/c. The differential cross section was converted to the photoproduction channel by using detailed balance; the normalization factor was obtained from the first plot, since the effective beam flux was identical for both these measurements (the same data run was analyzed for the charge exchange as well as the radiative capture channels). In this plot, we also include existing data,<sup>3, 4, 5</sup> the SAID<sup>6</sup> prediction as well as the MAID<sup>7</sup> prediction.

### 3.2. Charge Exchange

The elusive charge exchange process has been the weakest link in partial-wave and coupled-channel studies. The accurate data that we obtained in this momentum region will help in improving the determinations of the isospin-odd s-wave scattering length, the  $\pi$ NN coupling constant, and the  $\pi$ -N  $\sigma$  term. In addition, better charge exchange data helps in evaluating the mass splitting of the  $\Delta$  - charge splitting of the  $P_{33}$  resonance and may result in new values for the  $P_{11}(1440)$  mass and width.

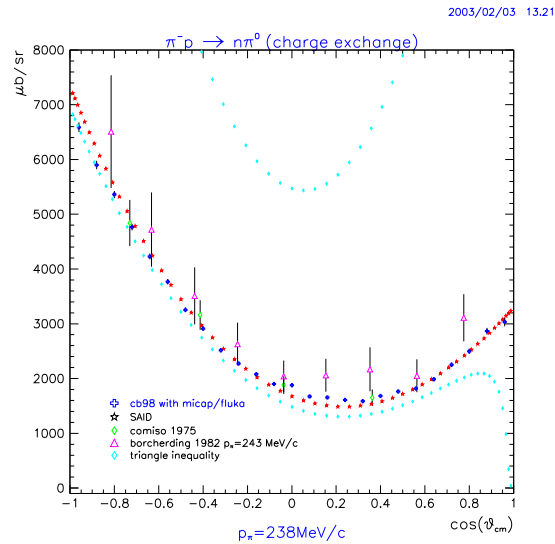


Figure 3. Our charge exchange differential cross section compared to previous measurements, <sup>4</sup>, <sup>8</sup> and the SAID <sup>9</sup> prediction at a pion beam momentum of 238 MeV/c. The triangle inequality sets upper and lower limits on the strength of charge exchange and is based on  $\pi^-p$  and  $\pi^+p$  elastic scattering data obtained from SAID.

Figure 3 shows the measured charge exchange differential cross section compared with the previously existing data, and the SAID <sup>9</sup> prediction at a pion beam momentum of 238 MeV/c. We also include the triangle inequality which sets upper and lower boundaries on the strength of charge exchange based on  $\pi^-p$  and  $\pi^+p$  elastic scattering data obtained from SAID. <sup>9</sup>

### 3.3. Two-Pion Production

Two pion production provides a means of studying sequential pion resonant decays; with neutral pions we study the  $\pi\pi$  interaction in the absence of final-state Coulomb effects and owing to isospin considerations there is no contribution of  $\rho$  decay. The study of this process on the proton ( $\pi^-p \rightarrow \pi^0\pi^0n$ ) is the subject of a recently completed Ph.D. thesis.<sup>10</sup> We have also published measurements on this process in the nuclear medium.<sup>11</sup>

### 3.4. Eta Production

Near threshold  $\eta$ -production measurements provides data<sup>12</sup> useful in verifying models of  $\eta$ -meson production and are also necessary for extraction of the  $\eta$ -N scattering length. Precise  $\eta$  production data are necessary to resolve ambiguities in the resonance properties of the  $S_{11}(1535)$  and in the  $\eta$  photoproduction helicity amplitudes.

## 4. Kaon-Induced Reactions

Using the Crystal Ball Detector, we have the ability of selecting pure isospin states. For example in the reactions  $K^-p \rightarrow \eta\Lambda$ <sup>13</sup> and  $K^-p \rightarrow \pi^0\Sigma^0$ , we select a pure  $I = 0$   $\Lambda^*$  and in the reaction  $K^-p \rightarrow \pi^0\Lambda$ , we select a  $I = 1$   $\Sigma^*$ . Figure 4 shows the production cross section of the former reaction. A significant part of our program is geared toward the study of  $K^-p$  reactions are described in a recent publication.<sup>14</sup>

## 5. Decays of the Eta

The large production cross section of tagged  $\eta$ s allow us to search for breaking of fundamental symmetries (*e.g.* C and CP invariance), and test Chiral Perturbation Theory as well as other theoretical models. We have published an article on  $\eta \rightarrow 4\pi^0$ <sup>15</sup> which presents a new upper limit for this branching ratio ( $B \leq 6.9 \times 10^{-7}$ ) of the CP forbidden decay at the 90% confidence level. This value of  $B$  puts a 2% limit on CP in quark-family-conserving interactions.

Another article has been published on the rare  $\eta \rightarrow 3\pi^0$ <sup>16</sup> which presents our determination of the quadratic slope parameter  $\alpha$  for that decay. The value obtained ( $\alpha = -0.031 \pm 0.004$ ) disagrees significantly with current theory. Since this published material is now readily available, I will discuss our recent and yet unpublished work on the  $\pi^0\gamma\gamma$  decay of the  $\eta$ .

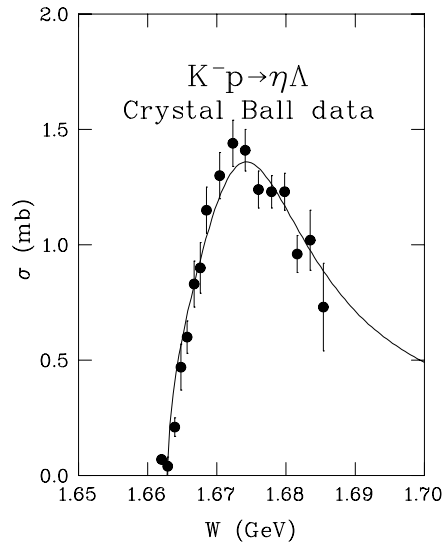


Figure 4. Total cross section for the reaction  $K^-p \rightarrow \eta\Lambda$ . Solid squares show cross section derived from  $\eta \rightarrow \gamma\gamma$  and the open squares are derived from the  $3\pi^0$  decay mode.

## 6. Rare Decays of the $\eta$ Meson

As we have alluded to above, by studying the rare and forbidden decay modes of the  $\eta$  meson, we are able to test the limits of such fundamental symmetries as C and CP invariance and G parity. Additionally, these also provide a laboratory in which we can test chiral perturbation theory and other recently proposed models. As mentioned above, some of these measurements are already in the literature.<sup>15 16</sup>

To measure the  $\eta$ -decay processes, we took a series of dedicated  $\pi^-p$  runs at 720 MeV/c which was at the maximum in eta production and yet close enough to threshold that the  $\eta$ s were essential going forward in the lab. In effect, we produced an  $\eta$  beam and use it to measure the eta decay channels.

For the decay  $\pi^-p \rightarrow \eta n \rightarrow \pi^0\gamma\gamma n$ , we looked at events in which 4 photons were detected. Even with this restriction, we still had backgrounds due to  $3\pi^0$  decay and direct  $2\pi^0$  production. These backgrounds were reduced by a series of kinematic checks which not only required that the 4 photons satisfied the kinematics of the desired final state, but also eliminated any events with even a small probability (0.1%) of satisfying the kinematics of possible background processes.



In addition to the above kinematic restrictions, we made various target and detector cuts that tested our abilities to Monte Carlo the acceptance and detection efficiencies. In all cases, we obtained results consistent within our statistical and estimated systematic uncertainties.

Our preliminary result for the  $\eta \rightarrow \pi^0\gamma\gamma$  decay branching ratio is  $3.2 \pm 0.9_{tot} \times 10^{-4}$ .<sup>17</sup> This is less than half of the current Particle Data Group value of  $7.1 \pm 1.4 \times 10^{-4}$  and disagrees by about 3-4 standard deviations. However, our experimental value does agree with the latest chiral perturbation theory calculations.

Using a similar analysis procedure, one of our colleagues has just reported an upper limit of the  $\eta \rightarrow \pi^0\pi^0\gamma$  branching ratio of  $5 \times 10^{-4}$  at the 90% confidence level.<sup>18</sup>

## 7. Summary

The Crystal Ball Program at BNL has producing a large number of high-quality results in a very short time period after data taking. We have put severe constraints on tests of chiral perturbation theory and the limitations of fundamental symmetries. Full and short reports as well as downloads of publications and conference contributions are available to the public on our Crystal Ball Collaboration web site.<sup>19</sup> While hoping to complete our planned experimental program at BNL, members of the collaboration have brought the Crystal Ball back to Europe, in particular to MAMI at Mainz, Germany where a exciting new program is about to begin.

## 8. The Collaboration

The new Crystal Ball Collaboration consists of B. Draper, S. Hayden, J. Huddleston, D. Isenhower, C. Robinson, and M. Sadler, *Abilene Christian University*, C. Allgower and H. Spinka, *Argonne National Laboratory*, J. Comfort, K. Craig, and A. Ramirez, *Arizona State University*, T. Kycia (deceased), *Brookhaven National Laboratory*, M. Clajus, A. Marusic, S. McDonald, B. M. K. Nefkens, N. Phaisangittisakul, and W. B. Tippens, *University of California at Los Angeles*, J. Peterson, *University of Colorado*, W. Briscoe, A. Shafi, and I. Strakovsky *George Washington University*, H. Staudenmaier, *Universität Karlsruhe*, D. M. Manley and J. Olmsted, *Kent State University*, D. Peaslee, *University of Maryland*, V. Abaev, V. Bekrenev, N. Kozlenko, S. Kruglov, A. Kulbardis, I. Lopatin, and A. Starostin, *Petersburg Nuclear Physics Institute*, N. Knecht, G. Lolos, and Z. Papandreou, *University of Regina*, I. Supek, *Rudjer Boskovic Institute*

and A. Gibson, D. Grosnick, D. D. Koetke, R. Manweiler, and S. Stanislaus, *Valparaiso University*.

## 9. Acknowledgements

The members of the Crystal Ball Collaboration are supported in part by the United States Department of Energy, the United States National Science Foundation, the National Sciences and Engineering Research Council of Canada, the Russian Ministry of Sciences, Volkswagen Stiftung and the George Washington University Research Enhancement Fund and Virginia Campus.

## References

1. Stanislaus, T.D.S., *et al.*, Nucl. Instrum. Methods A **462**, 463 (2001).
2. Briscoe, W.J. *et al.*, JLab proposal E-94-103.
3. Tran, M.T. *et al.*, Nucl. Phys. **A324**, 301 (1979).
4. Comiso, J.C. *et al.*, Phys. Rev. D **12**, 719 (1975).
5. Boucrot *et al.*, Nuovo Cim. **A18**, 635 (1973).
6. Arndt, R.A., Briscoe, W.J., Strakovsky, I.I., and Workman, R.L., Phys. Rev. C **66**, 055213 (2002).
7. Kamalov, S.S., Yang, S.N., Drechsel, D., Hanstein, O., and Tiator, L., Phys. Rev. C **64**, 032201 (2001).
8. Borcharding, F.O., Ph.D. Thesis, UCLA (1982).
9. Pavan, M.M., Arndt, R.A., Strakovsky, I.I., Workman, R.L., in *Proceedings of the 9th International Symposium on Meson-Nucleon Physics and the Structure of the Nucleon (MENU2001)*, Habezettl, H. and Briscoe, W.J., editors,  $\pi$ N Newsletter, **16**, 110 (2002).
10. Craig, K., Ph.D. Thesis, Arizona State University (2001).
11. Starostin, A., *et al.*, Phys. Rev. Lett. **85**, 5539 (2000).
12. Kozlenko, N.G. *et al.*, in *Hadron Spectroscopy (Hadron 2001)*, Protvino, Russia August 25 - September 1, 2001, edited by D. Amelin and A.M. Zaitsev, AIP Conf. Proc. **619**, 697 (2002).
13. Starostin, A. *et al.*, Phys. Rev. C **64**, 055205 (2001).
14. Manley, D.M. *et al.*, Phys. Rev. Lett. **88**, 012002 (2002).
15. Prakhov, S. *et al.*, Phys. Rev. Lett. **84**, 4802 (2000).
16. Tippens, W.B. *et al.*, Phys. Rev. Lett. **87**, 192001 (2001).
17. Prakhov, S., Proceedings of the III International Conference on Non-Accelerator New Physics (2001); Crystal Ball Report CB-01-008 (2001).
18. Prakhov, S., Crystal Ball Report CB-01-009 (2001).
19. <http://bmkn8.physics.ucla.edu>.